PERGAMON

International Journal of Solids and Structures 37 (2000) 4289–4307

INTERNATIONAL JOURNAL OF SOLIDS and STRUCTURES

www.elsevier.com/locate/ijsolstr

Cylindrical bending of angle-ply laminates subjected to different sets of edge boundary conditions

Xiao-Ping Shu[a], Kostas P. Soldatos[b,*]

[a]*Department of Mechanical Engineering, Huaihai Institute of Technology, Lianyungang, Jiangsu, 222005, China*
[b]*University of Nottingham, Pope Building, Nottingham NG7 2RD, UK*

Received 21 January 1999; in revised form 31 March 1999

Abstract

This paper extends the applicability of a new stress analysis method towards the accurate determination of the detailed stress distributions in angle-ply laminated plates subjected to cylindrical bending. As far as simply supported plates are concerned, this problem has an exact elasticity solution. Here however a simpler, two-dimensional, shear deformable, plate model is employed which, accompanied with an appropriate set of through-thickness shape functions, makes the new stress analysis method very accurate. Hence, the existing exact elasticity solution is used only for a further verification of the reliability of the new method, which is then used for a more detailed stress analysis study of certain monoclinic and angle-ply laminated plates subjected to realistic edge boundary conditions. It is also shown that the corresponding stress analysis of cross-ply laminated plates subjected to cylindrical bending is a particular case of the present analysis. © 2000 Elsevier Science Ltd. All rights reserved.

Keywords: Stress analysis; Angle-ply laminates; Cylindrical bending; Influence of boundary conditions; Refined plate theories

1. Introduction

In a short series of recent publications, Soldatos and Watson (1997a, 1997b, 1997c) proposed a new method for the accurate stress analysis of laminated composite structural elements. The method is based on a successful specification of the shape functions involved in a general, two-dimensional, plate (Soldatos, 1993a, 1993b, 1995) or shell (Soldatos and Timarci, 1993; Timarci and Soldatos, 1995) model, in a manner that represents very accurately the three-dimensional elasticity solution (if any) of a corresponding simply supported structural element (e.g., Pagano, 1969, 1970; Srinivas and Rao, 1970; Ye and Soldatos, 1994; Soldatos and Ye, 1995). Hence, away of the element edges, the stress prediction

* Corresponding author. Fax: +44-0115-951-3837.
E-mail address: kostas.soldatos@nottingham.ac.uk (K.P. Soldatos).

0020-7683/00/$ - see front matter
PII: S0020-7683(99)00144-4

is mainly influenced by the action of these shape functions whereas it is the boundary condition applied on the solution of the plate or shell governing equations that mainly dictates the stress distribution near the edges.

For instance, the shape functions involved in (Soldatos and Watson, 1997b, 1997c) were determined in such an accurate manner that the chosen one-dimensional beam and two-dimensional plate models, respectively, were capable to represent exactly the corresponding elasticity solutions (Pagano, 1969; Srinivas and Rao, 1970) for simply supported edges. At this point, one should also give credit to Levinson's (1984) similar but earlier attempt which, though resulted in describing a linearly elasticity problem by means of non-linear differential equations (see also Soldatos and Watson, (1997a)), it also achieved to get the corresponding elasticity solution (Pagano, 1969) for simply supported edges. Though very accurate when dealing with other sets of edge boundary conditions however, this new stress analysis method (Soldatos and Watson, 1997b, 1997c) is still approximate. Apart the set of the boundary conditions employed in this respect there are also several other factors that can affect the level of the method's accuracy, which may therefore vary. Such factors are the geometrical characteristics of the structural element, its material properties and the stacking pattern, the type of the problem considered (static, dynamic, etc.) and form of the applied external loading as well as the degree of approximation involved during the development of the two-dimensional plate or shell theory employed.

It should be understood, in this respect, that there is not a unique choice of shape functions that can accommodate satisfactorily a change to all of these factors. On the contrary, a change of any single one of them may well require the determination and use of a different set of shape functions. It appears therefore that further relevant developments, as well as the improvement of the method itself, are based on the formation of a catalogue containing sets of such shape functions each one of which will apply to a certain type or to a certain class of particular problems. The formation of such a catalogue should evidently start with structural elements that have relatively simple material and geometrical characteristics and could gradually continue towards single (or even assemblies of) structural elements the corresponding characteristics of which present an increasing degree of complexity. Being the first papers that made use of this new method, however, all of Soldatos and Watson, (1997a, 1997b, 1997c) dealt with relatively simple cases of straight beams or rectangular plates made of one or more specially orthotropic layers (Jones, 1975).

In more detail, Soldatos and Watson, (1997a) employed the general shear deformable plate theory, which is termed as the general five-degrees-of-freedom plate theory (G5DOFPT) and makes use of two shape functions only. On the other hand, both (Soldatos and Watson, 1997b, 1997c) were based on a corresponding plate theory which, by making use of six relevant degrees of freedom (G6DOFPT), accounts further for the effects of transverse normal deformation thus making use of three shape functions. It is only the later publication (Soldatos and Watson, 1997c), however, that outlines the manner in which all of the three shape functions involved in the G6DOFPT can be determined though relevant numerical results were not presented.

Soldatos and Watson (1997a) applied the method in connection with the cylindrical bending of cross-ply laminated plates (Pagano, 1969) in which the plane strain considerations involved necessitate the determination and use of one shape function only. In this respect, the analysis followed by Soldatos and Watson (1997a) was also found suitable for the accurate prediction of stresses in cross-ply laminated, shear deformable, beams subjected to different sets of edge boundary conditions. Based on these plane strain considerations, a more accurate investigation of the influence that the edge boundary conditions have on the stress distributions in cross-ply laminated beams (plates in cylindrical bending) was then performed by Soldatos and Watson (1997b, 1997c). However, the incorporation of the effects of both the transverse shear and the transverse normal deformation necessitated the determination and use of two shape functions for the numerical examples considered by Soldatos and Watson (1997b, 1997c).

The purpose of the present paper is to extend the applicability of the method towards the accurate determination of stresses in plates that are made of generally orthotropic or even monoclinic elastic layers (Jones, 1975) and are subjected to cylindrical bending conditions. Employing the steps followed by Soldatos and Watson (1997a), however in which the plate was made by specially orthotropic layers, the present investigation is based on the cylindrical bending problem of angle-ply laminated, simply supported plates, the exact elasticity solution of which is due to Pagano (1970). Despite the plane strain considerations involved, and in contrast with the corresponding solution that holds for cross-ply laminates (Pagano, 1969), both the in-plane displacement components are non-zero in this case, due to the monoclinic-type material arrangement. Hence, dependent on whether the G5DOFPT (Soldatos and Watson, 1997a) or its advanced analogue (G6DOFPT) that also accounts for the effects of transverse normal deformation (Soldatos and Watson, 1997c) is employed, there is a need for the determination of two or three shape functions, respectively. Among these two alternative plate models, this paper employs the relatively simpler but still very accurate one (G5DOFPT).

2. Cylindrical bending of angle-ply plates: the G5DOFPT model

Consider an elastic plate of thickness h and assume that its middle plane lies on the Oxy plane of a Cartesian co-ordinate system $Oxyz$ (the positive Oz axis is directed upwards). Consider further that the plate is of infinite extent in the y-direction, while it has a constant length, L, in the x-direction. Assume further that the plate is made of an arbitrary number, N, of monoclinic, linearly elastic layers and is subjected to the loading,

$$q(x) = q_m \sin(p_m x), \quad p_m = m\pi/L, \; m = 1,2,\ldots \tag{1}$$

which acts normally and upwards on its top lateral plane, $z = h/2$. This would be understood as being a simple harmonic in the corresponding Fourier sine-series expansion of any relevant loading distribution. Denote finally with U, V and W the plate displacement components along the x-, y- and z-directions, respectively, and employ the usual notation for the corresponding strain and stress components (see Eqs. (5), below).

Due to the off-axis material configuration (angle-ply lay-up), all the displacement, strain and stress components take non-zero values everywhere throughout the plate. Due however to the symmetries involved in both the geometrical and the loading characteristics, all these quantities are assumed independent of the y parameter and, therefore, all their partial derivatives with respect to y are zero. For this cylindrical bending problem, there is an exact, three-dimensional elasticity solution (Pagano, 1970) that holds if the following set of boundary conditions are imposed on both edges ($x = 0,\ L$) of the plate:

$$\sigma_x = \tau_{xy} = W = 0. \tag{2}$$

As already mentioned, however, the present analysis is based on the two-dimensional G5DOFPT, a brief but detailed description of which is outlined in by Soldatos and Watson (1997a). It is denoted at this point that the two-dimensional analogue (see Eqs. (14) below) of the set of boundary conditions (2) is clearly the one that is usually termed as the SS4 set of simply supported edge boundary conditions. In a close connection with the process followed by Soldatos and Watson (1997a), however, that SS4 set will be considered in this study for comparison purposes only with corresponding stress analysis results based on the aforementioned exact elasticity solution (Pagano 1970).

In the particular case that the elastic plate is made of one or more specially orthotropic layers (cross-ply lay-up) the V displacement component also vanishes. This is the case in which the corresponding exact, plane strain elasticity solution (Pagano, 1969) holds if the following set of boundary conditions are imposed on both edges, $x = 0,\ L$:

$$\sigma_x = W = 0. \tag{3}$$

It is precisely this problem to which the present stress analysis method has already been applied, successfully, by Soldatos and Watson (1997a) on the basis of the G5DOFPT, though the principal interest there was also focused to the influence of the different sets of edge boundary conditions. This discussion makes clear that the cylindrical bending problem of cross-ply plates (Pagano, 1969) is essentially a particular case of the more general problem considered by Pagano (1970). It should therefore be expected that, in precisely the same context, the analysis and results presented by Soldatos and Watson (1997a) should be obtained as a particular case of the present study.

Under these considerations, the present needs of the G5DOFPT suggest that the stress–strain relations in the kth layer of the plate ($k = 1,2,\ldots,N$) should be given as follows,

$$\left\{\sigma^{(k)}\right\} = \left[Q_1^{(k)}\right]\{\varepsilon\}, \qquad \left\{\tau^{(k)}\right\} = \left[Q_2^{(k)}\right]\{\gamma\} \tag{4}$$

where,

$$\{\sigma\}^{\mathrm{T}} = \{\sigma_x,\sigma_y,\tau_{xy}\}, \quad \{\tau\}^{\mathrm{T}} = \{\tau_{xz},\tau_{yz}\}$$

$$\{\varepsilon\}^{\mathrm{T}} = \{\varepsilon_x,\varepsilon_y,\gamma_{xy}\}, \quad \{\gamma\}^{\mathrm{T}} = \{\gamma_{xz},y_{yz}\} \tag{5}$$

Moreover, it is,

$$[Q_1] = \begin{bmatrix} Q_{11} & Q_{12} & Q_{16} \\ Q_{12} & Q_{22} & Q_{26} \\ Q_{16} & Q_{26} & Q_{66} \end{bmatrix}, \quad [Q_2] = \begin{bmatrix} Q_{55} & Q_{45} \\ Q_{45} & Q_{44} \end{bmatrix}, \tag{6}$$

where $Q_{ij}(i,j = 1,2,\ldots,6)$ denote the appropriate reduced elastic stiffnesses (Jones 1975).

Due to the symmetries involved in this cylindrical bending problem, the displacement approximation of the G5DOFPT is simplified as follows:

$$U(x,z) = u(x) - zw_{,x}(x) + \varphi_1(z)u_1(x),$$

$$V(x,z) = v(x) + \varphi_2(z)v_1(x),$$

$$W(x,z) = w(x), \tag{7}$$

but still contains all the five unknown degrees of freedom, u, v, w, u_1, and v_1, and therefore also involves both the shape functions, $\varphi_1(z)$ and $\varphi_2(z)$. Upon applying the kinematic relations of three-dimensional elasticity to the displacement approximation (7), one obtains the following approximate strain field:

$$\{\varepsilon\} = \{e^c\} + z\{\kappa^c\} + \left[\Phi(z)\right]\{\kappa^a\}, \quad \{\gamma\} = \left[\varphi'(z)\right]\left\{e_\gamma^a\right\}, \tag{8}$$

where,

$$\{\varepsilon\} = \begin{bmatrix} \varepsilon_x & \varepsilon_y & \gamma_{xy} \end{bmatrix}^{\mathrm{T}}, \quad \{e^c\} = \begin{bmatrix} u_{,x} & 0 & v_{,x} \end{bmatrix}^{\mathrm{T}}, \quad \{\kappa^c\} = \begin{bmatrix} -w_{,xx} & 0 & 0 \end{bmatrix}^{\mathrm{T}},$$

$$\{\kappa^a\} = \begin{bmatrix} u_{1,x} & 0 & v_{1,x} & 0 \end{bmatrix}^{\mathrm{T}}, \quad \{\gamma\} = \begin{bmatrix} \gamma_{xz} & \gamma_{yz} \end{bmatrix}^{\mathrm{T}}, \quad \{e_\gamma^c\} = \begin{bmatrix} u_1 & v_1 \end{bmatrix}^{\mathrm{T}},$$

$$[\Phi(z)] = \begin{bmatrix} \varphi_1(z) & 0 & 0 & 0 \\ 0 & 0 & 0 & \varphi_2(z) \\ 0 & \varphi_1(z) & \varphi_2(z) & 0 \end{bmatrix}, \quad [\varphi'(z)] = \begin{bmatrix} \varphi_1'(z) & 0 \\ 0 & \varphi_2'(z) \end{bmatrix}, \tag{9}$$

and a prime denotes ordinary differentiation with respect to z.

Moreover, the equations of equilibrium of the G5DOFPT are simplified as follows:

$$N_{x,x} = 0, \quad N_{xy,x} = 0,$$

$$M_{x,xx} = -q(x), \quad M^a_{x,x} - Q^a_x = 0, \quad M^a_{yx,x} - Q^a_y = 0, \tag{10}$$

where the force and moment resultants are still defined as follows:

$$(N_x, N_{xy}) = \int_{-h/2}^{h/2} (\sigma_x, \tau_{xy})\, \mathrm{d}z, \quad (M_x, M_{xy}) = \int_{-h/2}^{h/2} (\sigma_x, \tau_{xy}) z\, \mathrm{d}z,$$

$$(M^a_x, M^a_{yx}) = \int_{-h/2}^{h/2} \big(\sigma_x \varphi_1(z), \tau_{xy}\varphi_2(z)\big)\, \mathrm{d}z,$$

$$(Q^a_x, Q^a_y) = \int_{-h/2}^{h/2} \big(\tau_{xz}\varphi_1'(z), \tau_{yz}\varphi_2'(z)\big)\, \mathrm{d}z. \tag{11}$$

These definitions, in connection with Eqs. (6), (8) and (9), convert the equilibrium Eqs. (10) into the following form,

$$A_{11}u_{,xx} + A_{16}v_{,xx} + B_{111}u_{1,xx} + B_{162}v_{1,xx} - B_{11}w_{,xxx} = 0,$$

$$A_{16}u_{,xx} + A_{66}v_{,xx} + B_{161}u_{1,xx} + B_{662}v_{1,xx} - B_{16}w_{,xxx} = 0,$$

$$B_{11}u_{,xxx} + B_{16}v_{,xxx} + D_{111}u_{1,xxx} + D_{162}v_{1,xxx} - D_{11}w_{xxx} = -q(x),$$

$$B_{111}u_{,xx} + B_{161}v_{,xx} + D_{1111}u_{1,xx} + D_{1612}v_{1,xx} - A_{5511}u_1 - A_{4512}v_1 - D_{111}w_{,xxx} = 0,$$

$$B_{162}u_{,xx} + B_{662}v_{,xx} + D_{1612}u_{1,xx} + D_{6622}v_{1,xx} - A_{4512}u_1 - A_{4422}v_1 - D_{162}w_{,xxx} = 0, \tag{12}$$

where the stretching, coupling and bending rigidities are quoted from the following definitions (Timarci and Soldatos 1995):

$$A_{ij} = \int_{-h/2}^{h/2} Q_{ij}^{(k)}\, \mathrm{d}z, \quad A_{ijlm} = \int_{-h/2}^{h/2} Q_{ij}^{(k)} \varphi_l' \varphi_m'\, \mathrm{d}z, \quad B_{ij} = \int_{-h/2}^{h/2} Q_{ij}^{(k)} z\, \mathrm{d}z, \quad B_{ijl} = \int_{-h/2}^{h/2} Q_{ij}^{(k)} \varphi_l\, \mathrm{d}z,$$

$$D_{ij} = \int_{-h/2}^{h/2} Q_{ij}^{(k)} z^2 \, \mathrm{d}z, \quad D_{ijl} = \int_{-h/2}^{h/2} Q_{ij}^{(k)} \varphi_l z \, \mathrm{d}z, \quad D_{ijlm} = \int_{-h/2}^{h/2} Q_{ij}^{(k)} \varphi_l \varphi_m \, \mathrm{d}z, \tag{13}$$

by assigning appropriate indices.

Eq. (12) form a twelfth-order set of five simultaneous ordinary differential equations which, for a given appropriate set of the shape functions involved, can be solved for the five unknown displacement functions. Such an appropriate set of shape functions will be determined in the next section whereas the general solution of Eq. (12) will be obtained in Section 4. There, the manner will be further shown in which this solution can be associated to any set of boundary conditions that can be imposed on the two edges ($x = 0,L$) of the plate. Among the many different sets of such boundary conditions, it is however of particular interest to consider separately the following simply supported (SS4) set.

$$N_x = N_{xy} = w = M_x = M_x^a = M_{yx}^a = 0. \tag{14}$$

Upon taking the definitions (11) into consideration, this can be clearly shown to be the two-dimensional analogue of the corresponding three-dimensional set (2) used by Pagano (1970).

The SS4 set of boundary conditions (14) is satisfied exactly by a displacement choice of the form,

$$(u,u_1,v,v_1) = (A,B,C,D)\cos(p_m x), \quad w = E\sin(p_m x). \tag{15}$$

Moreover, it further satisfies exactly the set of the differential equations (12) in the sense that it converts it into the following set of simultaneous algebraic equations:

$$\begin{bmatrix} A_{11}p_m^2 & A_{16}p_m^2 & B_{111}p_m^2 & B_{162}p_m^2 & -B_{11}p_m^3 \\ & A_{66}p_m^2 & B_{161}p_m^2 & B_{662}p_m^2 & -B_{16}p_m^3 \\ & & D_{1111}p_m^2 + A_{5511} & D_{1612}p_m^2 + A_{4512} & -D_{111}p_m^3 \\ \text{Symmetric} & & & D_{6622}p_m^2 + A_{4422} & -D_{162}p_m^3 \\ & & & & D_{11}p_m^4 \end{bmatrix} \begin{Bmatrix} A \\ C \\ B \\ D \\ E \end{Bmatrix} = \begin{Bmatrix} 0 \\ 0 \\ 0 \\ 0 \\ q_m \end{Bmatrix}. \tag{16}$$

For any given set of shape functions $\varphi_1(z)$ and $\varphi_2(z)$, the integrations denoted in Eq. (13) can be performed either analytically or numerically. Hence, upon evaluating all the rigidities appearing in the algebraic Eq. (16), its unique solution will provide the values of the unknown constant coefficients A, B, C, D and E and, through Eqs. (15), (7), (8) and (4), the through-thickness distributions of the displacements, strains, and stresses. Hence, the main concern in accurately predicting these through-thickness distributions is the manner in which an appropriate set of shape functions $\varphi_1(z)$ and $\varphi_2(z)$ is determined.

3. Shape functions for cylindrical bending of angle-ply plates

Since the G5DOFPT neglects the effects of the transverse normal deformation, $\varphi_1(z)$ and $\varphi_2(z)$ are determined in this section by making use of the first and second of the three-dimensional equations of equilibrium only. For the cylindrical bending of angle-ply laminated plates, these equations are simplified as follows:

$$\sigma_{x,x} + \tau_{xz,z} = 0, \quad \tau_{xy,x} + \tau_{yz,z} = 0. \tag{17}$$

Using Hooke's law (6) in connection with Eqs. (8), (9) and (15), (17) yields the following fourth-order set of simultaneous ordinary differential equations,

$$Q_{55}^{(k)}\Phi_{1,zz}^{(k)} + Q_{45}^{(k)}\Phi_{2,zz}^{(k)} - Q_{11}^{(k)}p_m^2\Phi_1^{(k)} - Q_{16}^{(k)}p_m^2\Phi_2^{(k)} = Q_{11}^{(k)}p_m^2(A - zEp_m) + Q_{16}^{(k)}Cp_m^2, \tag{18a}$$

$$Q_{45}^{(k)}\Phi_{1,zz}^{(k)} + Q_{44}^{(k)}\Phi_{2,zz}^{(k)} - Q_{16}^{(k)}p_m^2\Phi_1^{(k)} - Q_{66}^{(k)}p_m^2\Phi_2^{(k)} = Q_{16}^{(k)}p_m^2(A - zEp_m) + Q_{66}^{(k)}Cp_m^2, \tag{18b}$$

where,

$$\Phi_1^{(k)}(z) = B\varphi_1^{(k)}(z), \quad \Phi_2^{(k)}(z) = D\varphi_2^{(k)}(z). \tag{19}$$

Here, the superscript (k) is associated with the shape functions in order to make it clear that, in general, their distribution changes from layer to layer. It may be of interest to note that in the particular case of a special orthotropic layer ($Q_{45}^{(k)} = Q_{16}^{(k)} = 0$) the set of differential equations (18) converts into two, uncoupled, second-order ordinary differential equations. Eq. (18a) takes then the form of the single, second-order, differential equation solved by Soldatos and Watson (1997a) for the determination of the single shape function needed when the cylindrical bending of cross-ply laminates is studied.

The general solution of Eq. (18) is given as follows ($k = 1,2,\ldots,N$):

$$\Phi_1^{(k)}(z) = \sum_{i=1}^{4} C_i^{(k)} e^{\alpha_i^{(k)} z} + Ep_m z - A, \tag{20a}$$

$$\Phi_2^{(k)}(z) = \sum_{i=1}^{4} \frac{Q_{55}^{(k)}\left(\alpha_i^{(k)}\right)^2 - Q_{11}^{(k)}p_m^2}{Q_{16}^{(k)}p_m^2 - Q_{45}^{(k)}\left(\alpha_i^{(k)}\right)^2} C_i^{(k)} e^{\alpha_i^{(k)} z} - C \tag{20b}$$

where $C_i^{(k)}$ represent four arbitrary constants of integration in the kth layer. The constants $\alpha_i^{(k)}$ ($i = 1,2,3,4$) are the four roots of the following quartic algebraic equation:

$$\left[Q_{44}^{(k)}Q_{55}^{(k)} - \left(Q_{45}^{(k)}\right)^2\right]\alpha^4 - \left(Q_{11}^{(k)}Q_{44}^{(k)} + Q_{66}^{(k)}Q_{55}^{(k)} - 2Q_{16}^{(k)}Q_{45}^{(k)}\right)p_m^2\alpha^2 + \left[Q_{11}^{(k)}Q_{66}^{(k)} - \left(Q_{16}^{(k)}\right)^2\right]p_m^4 = 0, \tag{21}$$

and, in general, differ from layer to layer.

It is of interest to further note that in the particular case of a special orthotropic layer ($Q_{45}^{(k)} = Q_{16}^{(k)} = 0$) the four roots of Eq. (21), which is quadratic in α^2, are as follows:

$$\alpha_{1,2}^{(k)} = \pm p_m\sqrt{\frac{Q_{11}^{(k)}}{Q_{55}^{(k)}}}, \quad \alpha_{3,4}^{(k)} = \pm p_m\sqrt{\frac{Q_{66}^{(k)}}{Q_{44}^{(k)}}}. \tag{22}$$

With Eq. (18) becoming uncoupled in that case, the two former of these roots are only associated with $\Phi_1^{(k)}(z)$, whereas the two later roots are associated with $\Phi_2^{(k)}(z)$. This observations clearly show that the single shape function obtained by Soldatos and Watson (1997a) is a particular case of the $\Phi_1^{(k)}(z)$ function given in Eq. (20a).

In a close relation to the corresponding results obtained by Soldatos and Watson (1997a), the right-hand sides of both Eqs. (18) are entirely dependent upon the displacement field of the classical plate theory, whereas the left-hand sides depend on the corresponding additional field that incorporates the effects of transverse shear deformation. In this connection, the summation that appears in the right-hand side of each one of Eqs. (20) represents the complementary solution to the corresponding of the Eq. (18)

whereas the remaining terms represent a particular integral. The interpretation of these results is therefore entirely analogous to the corresponding interpretation detailed by Soldatos and Watson (1997a).

In more detail, these later terms, which are all cancelled by setting $A = C = E = 0$, eliminate the inaccuracies superposed onto the solution of the equilibrium equation (17) by the displacement field of the classical plate theory. This is further clarified by the fact that, with a choice of the form (20), Eqs. (18) and therefore their equivalent elasticity Eq. (17) are satisfied regardless of the values of all the five unknown constants (A, B, C, D and E). As a result, for the cylindrical bending of simply supported, angle-ply plates, values can initially be assigned to all these unknown constants in an almost arbitrary manner. In doing so, the only essential requirement is that non-zero values should be assigned to both B and D, a nullification of which is equivalent to neglecting the effects of the transverse shear deformation.

Hence, provided that non-zero values are assigned to both B and D, any set of shape functions $\Phi_1(z)$ and $\Phi_2(z)$ produced by means of Eq. (20) exactly satisfies Eq. (17) of three-dimensional elasticity for this particular cylindrical bending problem of shear deformable, simply supported, angle-ply laminated plates. Despite that there is thus a complete freedom in choosing the values of all five of A, B, C, D and E, some convenient choice to four of them is made by employing the physical role that u, v, u_1, and v_1 are commonly required to play in G5DOFT. Namely, that u, v represent the in-plane displacements on the plate middle-plane ($z = 0$) whereas u_1, and v_1 depict the values of the transverse shear strains y_{xz} and y_{yz}, respectively, on that plane (Soldatos and Watson, 1997a). These requirements yield the following relationships,

$$A = \sum_{i=1}^{4} C_i^{(\mathrm{mp})}, \quad C = \sum_{i=1}^{4} \frac{Q_{55}^{(\mathrm{mp})}\left(\alpha_i^{(\mathrm{mp})}\right)^2 - Q_{11}^{(\mathrm{mp})} p_m^2}{Q_{16}^{(\mathrm{mp})} p_m^2 - Q_{45}^{(\mathrm{mp})}\left(\alpha_i^{(\mathrm{mp})}\right)^2} C_i^{(\mathrm{mp})},$$

$$D = \sum_{i=1}^{4} \frac{Q_{55}^{(\mathrm{mp})}\left(\alpha_i^{(\mathrm{mp})}\right)^2 - Q_{11}^{(\mathrm{mp})} p_m^2}{Q_{16}^{(\mathrm{mp})} p_m^2 - Q_{45}^{(\mathrm{mp})}\left(\alpha_i^{(\mathrm{mp})}\right)^2} \alpha_i^{(\mathrm{mp})} C_i^{(\mathrm{mp})},$$

$$E = \frac{1}{p_m}\left(B - \sum_{i=1}^{4} \alpha_i^{(\mathrm{mp})} C_i^{(\mathrm{mp})}\right). \tag{23}$$

Here, B is chosen to be the non-zero proportionality factor that, since its value leaves the final numerical results unaffected, can be left undetermined or set equal to unity without loss of generality (Soldatos and Watson 1997a). The index 'mp' indicates quantities that are associated with the layer that contains the plate middle-plane. In the particular case in which it coincides with a plate material interface, any one of the two layers bonded to that interface could be chosen to play the role of that 'middle-plane layer'.

For an N-layered plate, however, there are still $4N$ additional unknown constants to be determined, namely the $4N$ arbitrary constants of integration, $C_i^{(k)}$ ($i = 1,2,3,4$; $k = 1,2,\ldots,N$). These will be determined by means of the $4(N-1)$ continuity conditions employed on the $N-1$ material interfaces of the laminated plate considered and the four zero shear traction boundary conditions specified on the plate lateral planes. In more detail, upon requiring continuity of the in-plane displacement components, $U(x,z)$ and $V(x,z)$, at the kth material interface, $z = z_k$, of the laminate, one obtains ($k = 1,2,\ldots,N-1$),

$$\Phi_1^{(k)}(z_k) - \Phi_2^{(k+1)}(z_k) = 0, \quad \Phi_2^{(k)}(z_k) - \Phi_2^{(k+1)}(z_k) = 0. \tag{24}$$

Upon requiring continuity of the interlaminar shear stress at the same interface, one obtains further ($k = 1,2,\ldots,N-1$),

$$Q_{55}^{(k)}\Phi_{1,z}^{(k)}(z_k) + Q_{45}^{(k)}\Phi_{2,z}^{(k)}(z_k) - Q_{55}^{(k+1)}\Phi_{1,z}^{(k+1)}(z_k) - Q_{45}^{(k-1)}\Phi_{2,z}^{(k+1)}(z_k) = 0,$$

$$Q_{45}^{(k)}\Phi_{1,z}^{(k)}(z_k) + Q_{44}^{(k)}\Phi_{2,z}^{(k)}(z_k) - Q_{45}^{(k+1)}\Phi_{1,z}^{(k+1)}(z_k) - Q_{44}^{(k-1)}\Phi_{2,z}^{(k+1)}(z_k) = 0. \tag{25}$$

A requirement of zero shear tractions on the plate lateral planes, $z = \pm h/2$, yields finally,

$$Q_{55}^{(1)}\Phi_{1,z}^{(1)}(-h/2) + Q_{45}^{(1)}\Phi_{2,z}^{(1)}(-h/2) = 0,$$

$$Q_{45}^{(1)}\Phi_{1,z}^{(1)}(-h/2) + Q_{44}^{(1)}\Phi_{2,z}^{(1)}(-h/2) = 0,$$

$$Q_{55}^{(N)}\Phi_{1,z}^{(N)}(h/2) + Q_{45}^{(N)}\Phi_{2,z}^{(N)}(h/2) = 0,$$

$$Q_{45}^{(N)}\Phi_{1,z}^{(N)}(h/2) + Q_{44}^{(N)}\Phi_{2,z}^{(N)}(h/2) = 0. \tag{26}$$

Eqs. (24)–(26) form a set of $4N$ linear algebraic equations, the solution of which will determine the numerical values of the same number of unknowns $C_i^{(k)}$ ($i = 1,2,3,4$; $k = 1,2,\ldots,N$).

4. Angle-ply plates subjected to general boundary condition

Regardless of the particular form of the shape functions employed, the general solution of the ordinary differential Eq. (12) can be written as follows:

$$u = \sum_{i=1}^{4}(E_1E_{7i} + E_2E_{8i} + E_5\mu_i)K_ie^{\mu_i x} + K_9 + K_{10}x + E_5K_8x^2 + A\cos p_m x,$$

$$v = \sum_{i=1}^{4}(E_3E_{7i} + E_4E_{8i} + E_6\mu_i)K_ie^{\mu_i x} + K_{11} + K_{12}x + E_6K_8x^2 + C\cos p_m x,$$

$$u_1 = \sum_{i=1}^{4}E_{7i}K_ie^{\mu_i x} + 2\frac{C_3A_{4422} - C_6A_{4512}}{A_{4422}A_{5511} - A_{4512}^2}K_8 + B\cos p_m x,$$

$$v_1 = \sum_{i=1}^{4}E_{8i}K_ie^{\mu_i x} + 2\frac{C_6A_{5511} - C_3A_{4512}}{A_{4422}A_{5511} - A_{4512}^2}K_8 + D\cos p_m x,$$

$$w = \sum_{i=1}^{4}K_ie^{\mu_i x} + K_5 + K_6x + K_7x^2 + \frac{1}{3}K_8x^3 + E\sin p_m x, \tag{27}$$

where K_i $(i=1,2,\ldots,12)$ are arbitrary constants of integration to be determined when a set of edge boundary conditions are specified. Moreover, μ_i $(i=1,2,3,4)$ are the four roots of the following quartic equation:

$$\begin{aligned}&(C_1C_5C_9+C_2C_6C_7+C_3C_4C_8-C_1C_6C_8-C_2C_4C_9-C_3C_5C_7)\mu^4\\&+[(C_3C_7-C_1C_9)A_{4422}+(C_6C_8-C_5C_9)A_{5511}\\&+(C_9C_2+C_9C_4-C_3C_8-C_6C_7)A_{4512}]\mu^2+C_9\left(A_{4422}A_{5511}-A_{4512}^2\right)=0,\end{aligned}\tag{28}$$

where,

$$\begin{aligned}&C_1=B_{111}E_1+B_{161}E_3+D_{1111},\quad C_2=B_{111}E_2+B_{161}E_4+D_{1612},\\&C_3=B_{111}E_5+B_{161}E_6-D_{111},\quad C_4=B_{162}E_1+B_{662}E_3+D_{1612},\\&C_5=B_{162}E_2+B_{662}E_4+D_{6622},\quad C_6=B_{162}E_5+B_{662}E_6-D_{162},\\&C_7=B_{11}E_1+B_{16}E_3+D_{111},\quad C_8=B_{11}E_2+B_{16}E_4+D_{162},\quad C_9=B_{11}E_5+B_{16}E_6-D_{11},\end{aligned}\tag{29}$$

and,

$$\begin{aligned}&E_1=\frac{A_{16}B_{161}-A_{66}B_{111}}{A_{11}A_{66}-A_{16}^2},\quad E_2=\frac{A_{16}B_{662}-A_{66}B_{162}}{A_{11}A_{66}-A_{16}^2},\quad E_3=\frac{A_{16}B_{111}-A_{11}B_{161}}{A_{11}A_{66}-A_{16}^2},\\&E_4=\frac{A_{16}B_{162}-A_{11}B_{662}}{A_{11}A_{66}-A_{16}^2},\quad E_5=\frac{A_{66}B_{11}-A_{16}B_{16}}{A_{11}A_{66}-A_{16}^2},\quad E_6=\frac{A_{11}B_{16}-A_{16}B_{11}}{A_{11}A_{66}-A_{16}^2},\\&E_{7i}=\frac{C_6\left(C_2\mu_i^2-A_{4512}\right)-C_3\left(C_5\mu_i^2-A_{4422}\right)}{\left(C_1\mu_i^2-A_{5511}\right)\left(C_5\mu_i^2-A_{4422}\right)-\left(C_2\mu_i^2-A_{4512}\right)\left(C_4\mu_i^2-A_{4512}\right)},\\&E_{8i}=\frac{C_3\left(C_4\mu_i^2-A_{4512}\right)-C_6\left(C_1\mu_i^2-A_{5511}\right)}{\left(C_1\mu_i^2-A_{5511}\right)\left(C_5\mu_i^2-A_{4422}\right)-\left(C_2\mu_i^2-A_{4512}\right)\left(C_4\mu_i^2-A_{4512}\right)}.\end{aligned}\tag{30}$$

The remaining constants, A, B, C, D and E, that appear in Eq. (28) are the coefficients of terms that represent particular integrals of the set of Eq. (12). As such, these terms are identical to the solution (15) of the simply supported plate obtained by solving the linear algebraic system (16). In this respect, it is a rather simple matter to show that, for simply supported plates, the set of SS4 edge boundary conditions (14) yields zero values to all the arbitrary constants of integration, K_i $(i=1,2,\ldots,12)$, thus leaving Eq. (27) identical to Eq. (15). For plates subjected to a different set of edge boundary conditions, corresponding values to those constants are determined by applying that set of boundary conditions to Eq. (27) and, then, by solving the resulting 12×12 system of algebraic equations on the basis of a standard numerical routine.

5. Numerical results and discussion

In this section, the present analysis is initially applied to the cylindrical bending problem of angle-ply laminated plates, both edges of which are subjected to the SS4 set of simply supported boundary conditions (14). This case of simply supported plates is evidently used to test the reliability of the analysis, by comparing its results against corresponding numerical results based on the existing exact elasticity solution (Pagano, 1970). Hence, after the reliability of the method has successfully been tested, two further cases of angle-ply plates subjected to different sets of boundary conditions are considered, presenting stress analysis results that are entirely new in the literature. These cases are: (i) both edges rigidly clamped (CC plates), and (ii) one edge rigidly clamped and the other free of tractions (CF plates). In this respect, the following boundary conditions are imposed:

$$\text{at a clamped edge:} \quad u = v = w = w_{,x} = u_1 = v_1 = 0,$$

$$\text{at a free edge:} \quad N_x = N_{xy} = M_x = M_{x,x} = M_x^a = M_{yx}^a = 0. \tag{31}$$

It could be mentioned that, in the particular case of cross-ply laminates and upon inverting the direction of the applied loading, the present analysis produced identical results to those presented and discussed by Soldatos and Watson (1997a).

All the numerical results shown in what follows are presented by means of the following non-dimensional parameters:

$$\bar{U} = UE_{\mathrm{T}}/q_m L, \quad \bar{w} = 100wE_{\mathrm{T}}h^3/q_m L^4,$$

$$\left(\bar{\sigma}_x, \bar{\sigma}_y, \bar{\tau}_{xy}\right) = (\sigma_x, \sigma_y, \tau_{xy})h^2/q_m L^2,$$

$$\left(\bar{\tau}_{xz}, \bar{\tau}_{yz}\right) = (\tau_{xz}, \tau_{yz})h/q_m L, \tag{32}$$

and refer to homogeneous generally orthotropic plates as well as to two-layered plates having a regular antisymmetric angle-ply lay-up (Jones, 1975). The orthotropic material used in all of the applications employed has the following elastic properties:

$$E_{\mathrm{L}}/E_{\mathrm{T}} = 25, \quad G_{\mathrm{LT}}/E_{\mathrm{T}} = 0.5, \quad G_{\mathrm{TT}}/E_{\mathrm{T}} = 0.2, \quad \nu_{\mathrm{LT}} = \nu_{\mathrm{TT}} = 0.25, \tag{33}$$

where the subscripts L and T denote properties associated with the longitudinal and the transverse fibre direction, respectively. The integer value m that characterises the particular harmonic employed in the Fourier sine-series expansion of any loading distribution applied on the top lateral plane (Eq. (1)) is assumed to be unity. The plate geometry is mainly determined by the ratio $h/L = 0.25$. This characterises a very thick plate and, in conjunction with the high value of the stiffness ratio $E_{\mathrm{L}}/E_{\mathrm{T}}$, is considered to be an adequate test of the reliability of the method at least as far as simply supported plates are concerned. However, some cases of thinner plates have also been considered.

For several values of both the thickness to axial length ratio and the angle, θ, that the fibres form with the x-axis of a homogeneous SS4 plate, Table 1 presents the maximum values of the most important displacement and stress parameters predicted by means of the present analysis. Table 1 also compares these values with corresponding results that, based on the exact elasticity solution (Pagano, 1970), were tabulated by Ren (1986). Regardless of the fibre orientation, these comparisons show an excellent agreement of corresponding results which, as was expected, is particularly impressive in the case of the very thin plates ($h/L = 0.01$). This is due to the fact that the transverse normal deformation is essentially negligible in thin plates. Hence, like the G5DOFPT that completely ignores the effects of the transverse normal deformation, the exact elasticity solution predicts through-thickness displacement and stress distributions that are practically either symmetric or antisymmetric with respect to the plate middle-plane.

Even in the case of the very thick plates, in which the exact elasticity solution makes evident that the transverse normal deformation matters, an extremely good agreement is observed between corresponding numerical results, the relative discrepancy of which essentially never exceeds 3%. As an exception to this observation, the maximum value of the bending stress, σ_x, might be made reference to, for which the relative discrepancy of corresponding results for $h/L = 0.25$ and $\theta = 15^\circ$ is about 3.1%. It should be mentioned however that this value is always between the corresponding minimum and maximum values obtained by means of the exact elasticity ($z = \pm h/2$). Moreover, due to the fact that the axial plate reinforcement is decreasing by increasing the value of θ, this slight discrepancy also decrease with increasing θ. It is denoted in this respect, that in the case of a homogeneous plate made by specially orthotropic material ($\theta = 0^\circ$) the corresponding relative discrepancy observed was as high as 4.5% (Soldatos and Watson, 1997a), though it did not exceed the engineering acceptable error (5%). It should be finally emphasised that, regardless of the plate thickness, there is always an excellent agreement between the corresponding transverse shear stress distributions, τ_{xz} and τ_{yz}, obtained by means of the present analysis and the exact elasticity solution.

The particularly good performance of the present analysis is further shown in Table 2, where corresponding successful comparisons of complete through thickness stress distributions are performed for the case of $\theta = 15^\circ$. These comparisons show that, apart a narrow zone around the plate middle plane, in which however the stress values are small and therefore relatively less important, the above 3% discrepancy barrier is not exceeded. Moreover, similarly good results are presented in Tables 3 and 4, where corresponding comparisons to those shown in Tables 1 and 2, respectively, are performed for the case of a two-layered antisymmetric angle-ply laminated plate subjected to SS4 conditions. Having thus verified the good performance of the method, all of the remaining results shown in what follows deal

Table 1
Normalised displacement and stress parameters for homogeneous SS4 plates

h/L	θ	Exact					Present			
		$\bar{w}(L/2,0)$	$\bar{\sigma}_x(L/2,-h/2)$	$\bar{\sigma}_x(L/2,h/2)$	$\bar{\tau}_{yz}$ (0,0)	$\bar{\tau}_{xz}$ (0, 0)	$\bar{w}$ (L/2, 0)	$\bar{\sigma}_x(L/2,\pm h/2)$	$\bar{\tau}_{yz}$ (0,0)	$\bar{\tau}_{xz}$ (0,0)
0.25	15°	2.1089	−0.8338	0.8810	−0.1019	0.4353	2.1310	±0.8537	−0.1036	0.4360
	30°	2.6948	−0.7926	0.8264	−0.2127	0.4425	2.7230	±0.8086	−0.2160	0.4427
	45°	4.1681	−0.7314	0.7497	−0.3326	0.4535	4.2117	±0.7422	−0.3372	0.4533
	60°	7.8569	−0.6671	0.6745	−0.3975	0.4656	7.9382	±0.6734	−0.4025	0.4652
	75°	14.095	−0.6353	0.6388	−0.1809	0.4719	14.237	±0.6397	−0.1828	0.4714
0.10	15°	0.8162	−0.6560	0.6536	−0.1170	0.4689	0.8178	±0.6532	−0.1173	0.4688
	30°	1.1498	−0.6434	0.6445	−0.2454	0.4705	1.1521	±0.6444	−0.2459	0.4705
	45°	2.1366	−0.6312	0.6318	−0.3884	0.4729	2.1408	±0.6320	−0.3892	0.4728
	60°	5.2662	−0.6187	0.6189	−0.4696	0.4753	5.2763	±0.6193	−0.4706	0.4752
	75°	11.324	−0.6125	0.6126	−0.1891	0.4765	11.345	±0.6131	−0.1895	0.4765
0.01	15°	0.5629	−0.6082	0.6082	−0.1207	0.4772	0.5631	±0.6084	−0.1207	0.4774
	30°	0.8448	−0.6080	0.6080	−0.2531	0.4772	0.8452	±0.6083	−0.2532	0.4774
	45°	1.7277	−0.6077	0.6077	−0.4017	0.4770	1.7292	±0.6082	−0.4020	0.4774
	60°	4.7348	−0.6068	0.6068	−0.4871	0.4765	4.7448	±0.6080	−0.4881	0.4774
	75°	10.756	−0.6056	0.6056	−0.1903	0.4756	10.798	±0.6080	−0.1910	0.4774

Table 2
Through-thickness stress distributions in a SS4 homogeneous plate ($h/L = 0.25$, $\theta = 15°$)

z/h	Exact					Present				
	$\bar{\sigma}_x$ $(L/2)$	$\bar{\sigma}_y$ $(L/2)$	$\bar{\tau}_{xy}$ $(L/2)$	$\bar{\tau}_{yz}$ (0)	$\bar{\tau}_{xz}$ (0)	$\bar{\sigma}_x$ $(L/2)$	$\bar{\sigma}_y$ $(L/2)$	$\bar{\tau}_{xy}$ $(L/2)$	$\bar{\tau}_{yz}$ (0)	$\bar{\tau}_{xz}$ (0)
−0.5	−0.8338	−0.0651	0.2022	0.0000	0.0000	−0.8537	−0.0667	0.2088	0.0000	0.0000
−0.4	−0.4868	−0.0374	0.1151	−0.0486	0.2027	−0.4948	−0.0386	0.1186	−0.0502	0.2069
−0.3	−0.2809	−0.0200	0.0645	−0.0761	0.3205	−0.2817	−0.0219	0.0659	−0.0784	0.3260
−0.2	−0.1550	−0.0086	0.0347	−0.0913	0.3875	−0.1516	−0.0118	0.0347	−0.0938	0.3925
−0.1	−0.0730	−0.0004	0.0161	−0.0991	0.4227	−0.0661	−0.0051	0.0148	−0.1014	0.4259
0.0	−0.0087	0.0066	0.0022	−0.1019	0.4353	0.0000	0.0000	0.0000	−0.1036	0.4361
0.1	0.0570	0.0137	−0.0121	−0.1004	0.4280	0.0661	0.0051	−0.0148	−0.1014	0.4259
0.2	0.1444	0.0233	−0.0320	−0.0937	0.3942	0.1516	0.0118	−0.0347	−0.0938	0.3925
0.3	0.2798	0.0346	−0.0642	−0.0790	0.3323	0.2817	0.0219	−0.0659	−0.0784	0.3260
0.4	0.5034	0.0533	−0.1192	−0.0510	0.2123	0.4948	0.0386	−0.1186	−0.0502	0.2069
0.5	0.8810	0.0835	−0.2140	0.0000	0.0000	0.8537	0.0667	−0.2088	0.0000	0.0000

with two-layered plates having both their edges clamped or one edge clamped and the other free of tractions.

Table 5 presents numerical values of normalised displacement and stresses at selected points within a CC plate having a [30°/−30°] lay-up. It should be noted that, due to the symmetries of the problem, displacement and stresses at x/L and $1 - x/L$ have identical through-thickness distributions. Moreover, due to the G5DOFPT considerations, they are also either symmetric or antisymmetric with respect to the plate middle plane. Hence, numerical results are only presented for the left half of the top layer of the CC plate. The fundamental difference observed between associated through-thickness displacement and stress distributions in corresponding SS4 and CC cross-ply laminated plates (Soldatos and Watson, 1997a) becomes also evident in the present case that deals with angle-ply laminates. Due to their

Table 3
Normalised displacement and stress parameters of SS4 two-layered plates $[-\theta/\theta]$

h/L	θ	Exact					Present			
		$\bar{w}(L/2,0)$	$\bar{\sigma}_x(L/2,-h/2)$	$\bar{\sigma}_x(L/2,h/2))$	$\bar{\tau}_{yz}(0,0)$	$\bar{\tau}_{xz}(0,0)$	$\bar{w}(L/2,0)$	$\bar{\sigma}_x(L/2 \pm h/2)$	$\bar{\tau}_{yz}(0,0)$	$\bar{\tau}_{xx}(0,0)$
0.25	15°	2.662	−0.9966	1.0439	−0.0028	0.2884	2.688	±1.0206	0.0000	0.2866
	30°	3.920	−1.0141	1.0789	−0.0057	0.2174	3.958	±1.0661	0.0000	0.2143
	45°	6.287	−0.9601	0.9798	−0.0085	0.2513	6.346	±0.9758	0.0000	0.2484
	60°	10.686	−0.7876	0.7958	−0.0096	0.3606	10.789	±0.7962	0.0000	0.3589
	75°	14.966	−0.6513	0.6548	−0.0036	0.4589	15.115	±0.6559	0.0000	0.4582
0.10	15°	1.441	−0.8700	0.8716	−0.0005	0.2953	1.443	±0.8719	0.0000	0.2931
	30°	2.530	−0.9671	0.9682	−0.0010	0.2107	2.535	±0.9690	0.0000	0.2101
	45°	4.483	−0.9150	0.9156	−0.0016	0.2455	4.590	±0.9166	0.0000	0.2450
	60°	8.512	−0.7578	0.7580	−0.0019	0.3641	8.528	±0.7588	0.0000	0.3637
	75°	12.141	−0.6278	0.6279	−0.0007	0.4645	12.163	±0.6284	0.0000	0.4644
0.01	15°	1.205	−0.8402	0.8402	0.0000	0.2945	1.206	±0.8409	0.0000	0.2948
	30°	2.262	−0.9485	0.9485	0.0000	0.2089	2.265	±0.9498	0.0000	0.2091
	45°	4.249	−0.9033	0.9033	0.0000	0.2436	4.258	±0.9052	0.0000	0.2441
	60°	8.071	−0.7488	0.7488	0.0000	0.3635	8.100	±0.7515	0.0000	0.3648
	75°	11.555	−0.6205	0.6205	0.0000	0.4636	11.603	±0.6231	0.0000	0.4656

Table 4
Through-thickness stress distributions in a SS4 two-layered plate ($l/h = 0.25$, [-15°/15°])

z/h	Exact					Present				
	$\bar{\sigma}_x(L/2)$	$\bar{\sigma}_y(L/2)$	$\bar{\tau}_{xy}(L/2)$	$\bar{\tau}_{yz}(0)$	$\bar{\tau}_{xz}(0)$	$\bar{\sigma}_x(L/2)$	$\bar{\sigma}_y(L/2)$	$\bar{\tau}_{xy}(L/2)$	$\bar{\tau}_{yz}(0)$	$\bar{\tau}_{xz}(0)$
−0.5	−0.9966	−0.0714	0.2026	0.0000	0.0000	−1.0206	−0.0783	0.2116	0.0000	0.0000
−0.4	−0.5491	−0.0408	0.0935	−0.0457	0.2373	−0.5582	−0.0421	0.0950	−0.0467	0.2423
−0.3	−0.2579	−0.0166	0.0206	−0.0210	0.3612	−0.2580	−0.0185	0.0195	−0.0640	0.3676
−0.2	−0.0371	0.0025	−0.0346	−0.0605	0.4066	−0.0310	−0.0008	−0.0378	−0.0609	0.4120
−0.1	0.1785	0.0213	−0.0892	−0.0412	0.3851	0.1898	0.0166	−0.0942	−0.0403	0.3877
0.0	0.4529	0.0444	−0.1597	−0.0028	0.2884	0.4697	0.0385	−0.1667	0.0000	0.2866
0.0	−0.4716	−0.0315	−0.1684	−0.0028	0.2884	−0.4697	−0.0385	−0.1667	0.0000	0.2866
0.1	−0.1949	−0.0082	−0.0970	0.0383	0.3906	−0.1898	−0.0166	−0.0942	0.0403	0.3877
0.2	0.0262	0.0111	−0.0408	0.0597	0.4166	0.0310	0.0008	−0.0378	0.0609	0.4120
0.3	0.2570	0.0310	0.0170	0.0637	0.3732	0.2580	0.0185	0.0198	0.0640	0.3676
0.4	0.5660	0.0567	0.0943	0.0470	0.2470	0.5582	0.0421	0.0950	0.0467	0.2423
0.5	1.0439	0.0948	0.2148	0.0000	0.0000	1.0206	0.0783	0.2116	0.0000	0.0000

Table 5
Displacement and stress distributions in a CC two-layered plate ($h/L = 0.25$, [−30°/30°])

	z/h	$x/L = 0.0$	0.1	0.2	0.3	0.4	0.5
$\bar{w}$		0.0000	0.4596	1.0633	1.5834	1.9323	2.0549
$\bar{\sigma}_x$	0.5	−2.2604	−0.2903	0.0246	0.2590	0.4098	0.4618
	0.4	−0.0536	−0.2038	−0.0454	0.0852	0.1694	0.1985
	0.3	0.3708	−0.1050	−0.0384	0.0193	0.0562	0.0689
	0.2	0.0338	0.0023	0.0012	−0.0022	−0.0050	−0.0061
	0.1	−0.2083	0.1149	0.0365	−0.0325	−0.0774	−0.0930
	0.0	0.5376	0.2296	0.0286	−0.1274	−0.2269	−0.2612
$\bar{\sigma}_y$	0.5	−0.6993	−0.0869	0.0081	0.0789	0.1245	0.1402
	0.4	0.0023	−0.0594	−0.0143	0.0237	0.0481	0.0565
	0.3	0.1323	−0.0281	−0.0117	0.0031	0.0125	0.0157
	0.2	0.0200	0.0060	0.0012	−0.0034	−0.0066	−0.0077
	0.1	−0.0587	0.0419	0.0125	−0.0130	−0.0295	−0.0353
	0.0	0.1842	0.0786	0.0098	−0.0436	−0.0777	−0.0895
$\bar{\tau}_{xz}$	0.5	0.0000	0.0000	0.0000	0.0000	0.0000	0.0000
	0.4	0.0000	0.2385	0.2067	0.1504	0.0791	0.0000
	0.3	0.0000	0.3619	0.3131	0.2277	0.1198	0.0000
	0.2	0.0000	0.3970	0.3427	0.2491	0.1310	0.0000
	0.1	0.0000	0.3499	0.3007	0.2182	0.1147	0.0000
	0.0	0.0000	0.2072	0.1756	0.1267	0.0664	0.0000
$\bar{U}$	0.5	0.0000	−0.1404	−0.1670	−0.1421	−0.0806	0.0000
	0.4	0.0000	−0.0722	−0.0991	−0.0886	−0.0513	0.0000
	0.3	0.0000	−0.0438	−0.0654	−0.0600	−0.0351	0.0000
	0.2	0.0000	−0.0342	−0.0479	−0.0431	−0.0250	0.0000
	0.1	0.0000	−0.0257	−0.0314	−0.0269	−0.0153	0.0000
	0.0	0.0000	0.0000	0.0000	0.0000	0.0000	0.0000

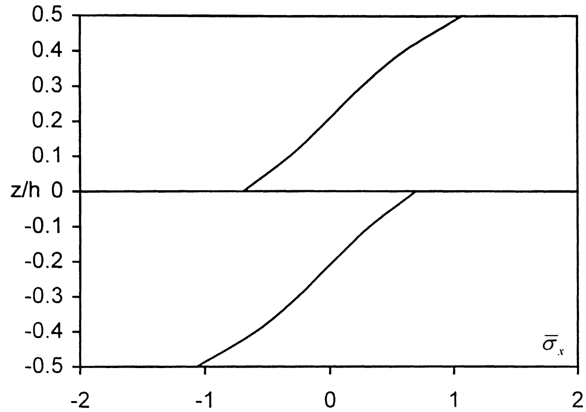

Fig. 1. Bending stress distribution in a [30°/−30°] SS plate.

trigonometric in-plane pattern (Eq. (15)), such through-thickness distributions in SS4 plates exhibit a certain similarity with respect to x, with the value of the trigonometric term simply affecting their magnitude only. On the contrary, the through-thickness displacement and stress distributions in a CC plate are very strongly dependent on the value of the in-plane co-ordinate x/L.

For instance, the form of the bending stress distribution, σ_x, is similar to that presented in Fig. 1, for $x/L = 0.5$, throughout the entire length of the SS4 plate, with an exception at the two edges of the plate at which it is identically zero. Contrary to this, the through-thickness bending stress distribution at the edges of a CC plate (solid line in Fig. 3) is highly non-linear, and takes particularly high values either close to the lateral planes ($z = \pm h/2$) or near the material interface ($z = 0$). Away from the edges ($x/L > 0.1$), the shape of the σ_x-distribution in a CC plate tends to gradually approach that of a corresponding SS4 plate.

Similar observations may be detailed with regard to the corresponding through-thickness distributions of the transverse shear stress τ_{xz} (Figs. 2 and 4), although the through-thickness distributions exhibit now a certain similarity, with respect, to x, even for CC plates. As has been also pointed out by Soldatos and Watson (1997a), however, although the magnitude of the τ_{xz}-distribution in a CC plate is naturally increasing when approaching the clamped edge ($\tau_{xz} = 0$ at $x/L = 0$), the present G5DOFPT

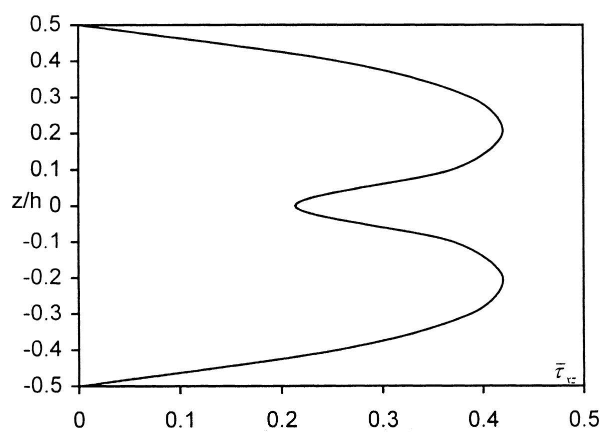

Fig. 2. Transverse shear stress distribution in a [30°/−30°] SS plate.

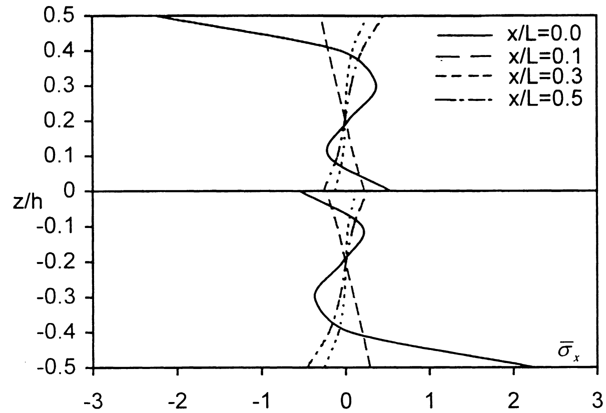

Fig. 3. Transverse shear stress distribution in a [30°/−30°] CC plate.

theory erroneously predicts that τ_{xz} suddenly becomes zero at that edge. This slight drawback, which decreases and essentially vanishes by decreasing the plate thickness, is apparently due to the limitations of the G5DOFPT. As was initially detailed by Soldatos and Watson (1997a) and verified afterwards for cross-ply laminates (Soldatos and Watson, 1997a, 1997b), an apparent way to improve this drawback, which might be considerable in studying edge delamination, is to replace G5DOFPT with a theory that also accounts for transverse normal deformation effects. Such a change of the plate theory which, for the cylindrical bending problem of angle-ply laminated plates, would involve the appropriate determination of more than two inter-related shape functions, is beyond the scope of the present study.

Table 6 presents numerical values of normalised displacement and stress distributions at equally spaced points within CF plate having a [30°/−30°] lay-up. Due to the G5DOFPT considerations, these distributions occur in either symmetric or antisymmetric forms, with respect to the plate middle plane. Hence, numerical results are only presented for the top layer of the CF plate. For this plate, associated complete through-thickness distributions of bending and shear stresses are shown graphically in Figs. 5 and 6, respectively, using selected coordinate values across the plate length. In a close relation with the corresponding observation made by Soldatos and Watson (1997a) for the cross-ply laminated CF plate, the present solution varies rapidly to meet the boundary conditions imposed on the free edge of the

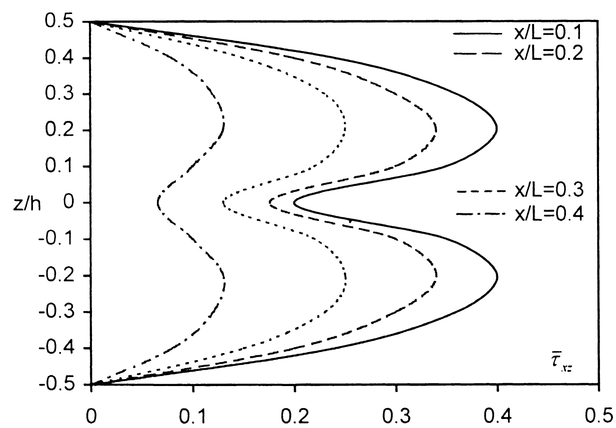

Fig. 4. Transverse shear stress distribution in a [30°/−30°] CC plate.

Table 6
Displacement and stress distributions in a CF two-layered plate ($h/L = 0.25$, [−30°/30°])

	z/h	$x/l = 0.0$	0.2	0.4	0.6	0.8	1.0
$\bar{w}$		0.0000	3.0330	7.6739	12.561	17.132	21.376
$\bar{\sigma}_x$	0.5	−6.3025	−1.7547	−0.7753	−0.1793	0.0300	0.0000
	0.4	−1.2682	−1.2129	−0.6082	−0.2170	−0.0417	0.0000
	0.3	0.1900	−0.5960	−0.3140	−0.1274	−0.0348	0.0000
	0.2	0.1217	0.0543	0.0323	0.0140	0.0042	0.0000
	0.1	0.2456	0.7031	0.3676	0.1440	0.0361	0.0000
	0.0	2.3547	1.3142	0.6264	0.1965	0.0200	0.0000
$\bar{\sigma}_y$	0.5	−1.9371	−0.5295	−0.2337	−0.0536	0.0094	0.0000
	0.4	−0.3359	−0.3565	−0.1801	−0.0653	−0.0133	0.0000
	0.3	0.1187	−0.1595	−0.0857	−0.0362	−0.0107	0.0000
	0.2	0.0872	0.0482	0.0253	0.0094	0.0020	0.0000
	0.1	0.1239	0.2553	0.1325	0.0511	0.0123	0.0000
	0.0	0.8066	0.4502	0.2146	0.0673	0.0068	0.0000
$\bar{\tau}_{xz}$	0.5	0.0000	0.0000	0.0000	0.0000	0.0000	0.0000
	0.4	0.0000	0.4640	0.3370	0.1788	0.0507	0.0018
	0.3	0.0000	0.7027	0.5099	0.2704	0.0765	0.0024
	0.2	0.0000	0.7687	0.5570	0.2951	0.0832	0.0023
	0.1	0.0000	0.6738	0.4870	0.2576	0.0722	0.0014
	0.0	0.0000	0.3919	0.2807	0.1478	0.0406	−0.0003
$\bar{U}$	0.5	0.0000	−1.0102	−1.4826	−1.6550	−1.6771	−1.6692
	0.4	0.0000	−0.7307	−1.1301	−1.2944	−1.3334	−1.3352
	0.3	0.0000	−0.5281	−0.8331	−0.9632	−0.9979	−1.0013
	0.2	0.0000	−0.3617	−0.5624	−0.6458	−0.6663	−0.6676
	0.1	0.0000	−0.1975	−0.2932	−0.3293	−0.3349	−0.3338
	0.0	0.0000	0.0000	0.0000	0.0000	0.0000	0.0000

angle-ply laminate in an almost point-by-point sense. In more detail, the bending stress is very large on the outer planes of the clamped edge ($x = 0$), on which its value is almost three times higher than the value that it takes at the edge of the corresponding, less flexible, CC plate (see Fig. 3). Similarly, in the vicinity of the clamped edge ($x/L = 0.1$) the through-thickness maximum value of the transverse shear

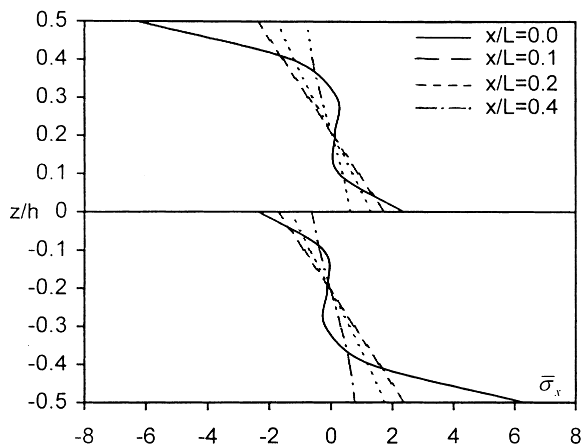

Fig. 5. Bending stress distribution in a [30°/−30°] CF plate.

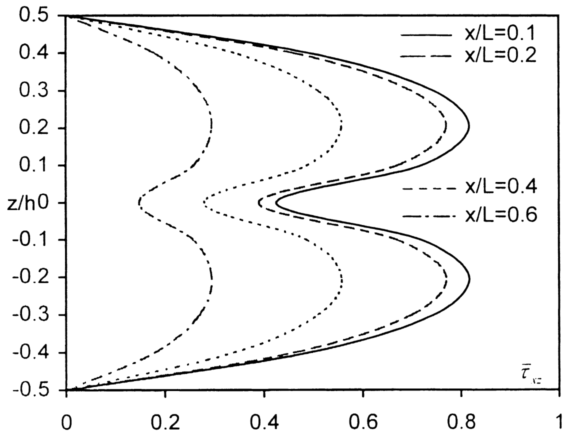

Fig. 6. Transverse shear stress distribution in a [30°/−30°] CF plate.

stress is about twice as high as it is for the corresponding CC plate (see Figs. 4 and 6). Most importantly, the zero bending stress boundary condition on the free edge ($x = L$) is satisfied exactly, in a point-by-point sense. This is not true with either of the transverse shear stress τ_{xz} and τ_{yz}, the values of which are however so small at $x = L$ that should practically be considered as zero.

6. Conclusions

A new stress analysis method that was demonstrated by Soldatos and Watson (1997a) for the cylindrical bending of cross-ply laminated plates has successfully been extended towards the accurate determination of the detailed stress distributions in angle-ply laminated plates subjected to cylindrical bending. Hence, the corresponding stress analysis presented by Soldatos and Watson (1997a) becomes a particular case of the present analysis, which is also based on the considerations of the G5DOFPT.

For angle-ply laminated plates subjected to a certain set of simply supported edge boundary conditions, the good performance of the present analysis has been verified by means of successful numerical comparisons performed with corresponding results based on the existing exact elasticity solutions (Pagano, 1970; Ren, 1986). New results have however also been presented with regard to the stress analysis of more realistically supported angle-ply laminated plates, namely for plates having one edge rigidly clamped and the other either rigidly clamped or free of external tractions. It should be noted, however, that the relevant analytical solution presented in Section 4 holds for any set of variationally consistent boundary conditions applied at the plate edges. Hence, if needed, the presented numerical analysis can successfully be repeated for other sets of edge boundary conditions, for which corresponding numerical results can also be obtained with ease.

The numerical results and comparisons performed for thin and moderately thick plates have shown an excellent performance of the present method. As far as thick plates are concerned ($h/L = 0.25$), the method still performs very reliably despite the limitations of the G5DOFPT. It is expected that the slight drawbacks observed (for thick plates only) may be improved by replacing the G5DOFPT with a plate theory that takes transverse normal deformation effects into consideration, in the sense described by Soldatos and Watson (1997b, 1997c) for the cylindrical bending of cross-ply laminates. It is denoted, however, that the additional degree of freedom involved in such a case will introduce a third shape function, which will be interconnected with both of the shape functions involved in the present analysis.

In such a case, the whole set of the three shape functions involved should appropriately be redetermined.

Acknowledgements

The authors are grateful to the Jiangsu Education Commission, China for sponsoring the research visit of X. Shu to the University of Nottingham.

References

Jones, R.M., 1975. Mechanics of Composite Materials. Hemisphere, New York.

Levinson, M., 1984. A novel approach to thick plate theory suggested by studies in foundation theory. International Journal of Mechanical Sciences 26, 427–436.

Pagano, N.J., 1969. Exact solution for composite laminates in cylindrical bending. Journal of Composite Materials 3, 398–411.

Pagano, N.J., 1970. Influence of shear coupling in cylindrical bending of anisotropic laminates. Journal of Composite Materials 4, 330–343.

Ren, J.G., 1986. Bending theory of laminated plate. Composites Science and Technology 27, 225–248.

Srinivas, S., Rao, A.K., 1970. Bending, vibration and buckling of simply supported thick orthotropic rectangular plates and laminates. International Journal of Solids and Structures 6, 1463–1481.

Soldatos, K.P., 1993a. Vectorial approach for the formulation of variationally consistent higher-order plate theories. Composites Engineering 3, 3–17.

Soldatos, K.P., 1993b. A non-linear transverse shear deformable plate theory allowing a multiple choice of trial displacement and stress distributions. Composites Engineering 3, 885–897.

Soldatos, K.P., 1995. Generalization of variationally consistent plate theories on the basis of a vectorial formulation. Journal of Sound and Vibration 183, 819–839.

Soldatos, K.P., Timarci, T., 1993. A unified formulation of aminated composite shear deformable five-degrees-of-freedom cylindrical shell theories. Composite Structures 25, 165–171.

Soldatos, K.P., Watson, P., 1997a. A method for improving the stress analysis performance of two-dimensional theories for composite laminates. Acta Mechanica 123, 163–186.

Soldatos, K.P., Watson, P., 1997b. A general four-degrees-of-freedom theory suitable for the accurate stress analysis of homogeneous and laminated composites beams. International Journal of Solids and Structures 34, 2857–2885.

Soldatos, K.P., Watson, P., 1997c. Accurate stress analysis of laminated plates combining a two-dimensional theory with the exact three-dimensional solution for simply supported edges. Mathematics and Mechanics of Solids 2, 459–489.

Soldatos, K.P., Ye, J.Q., 1995. Axisymmetric static and dynamic analysis of laminated hollow cylinders composed of monoclinic elastic layers. Journal of Sound and Vibration 184, 245–259.

Timarci, T., Soldatos, K.P., 1995. Comparative dynamic studies for symmetric cross-ply circular cylindrical shells on the basis of a unified shear deformable shell theory. Journal of Sound and Vibration 187, 609–624.

Ye, J.Q., Soldatos, K.P., 1994. Three-dimensional stress analysis of orthotropic and cross-ply laminated hollow cylinders and cylindrical panels. Computer Methods in Applied Mechanics and Engineering 117, 331–351.